RESEARCH PAPER

Utilization of Waste Tea-Derived CuO Nanoparticles to Enhance Visible Light Photocatalytic Decomposition of Rhodamine 6G Dye

Rehana Baiju Mampilly

Department of Science & Humanities, Government Polytechnic Kheda

Abstract

This study presents an eco-friendly and economical method for the synthesis of copper oxide nanoparticles (CuO NPs) using waste tea extract as a reducing and stabilizing agent. The synthesized waste tea-mediated CuO nanoparticles (WT-CuO NPs) were characterized by FTIR, XRD, FE-SEM, EDAX, and HR-TEM techniques. Copper oxide nanoparticles were synthesized through a green synthesis route utilizing waste tea extract. The photocatalytic degradation efficiency of the synthesized nanoparticles was evaluated using Rhodamine 6G dye under visible light and sunlight irradiation. The synthesized WT-CuO nanoparticles exhibited excellent photocatalytic activity toward Rhodamine 6G dye degradation. Under optimized conditions of pH 8, 50 ppm dye concentration, and 50 mg catalyst dosage, maximum degradation efficiency was observed under visible light irradiation within 90 minutes. The degradation efficiency under sunlight irradiation was also significant. The present study demonstrates that waste tea-mediated CuO nanoparticles are highly effective photocatalysts for the degradation of Rhodamine 6G dye. The green synthesized nanoparticles provide an environmentally sustainable and low-cost solution for wastewater treatment applications.

Keywords: Waste tea, CuO nanoparticles, Rhodamine 6G, photocatalytic degradation, visible light irradiation, green synthesis.

How to cite this article: Mampilly RB. Utilization of Waste Tea-Derived CuO Nanoparticles to Enhance Visible Light Photocatalytic Decomposition of Rhodamine 6G Dye. Int J Drug Deliv Technol. 2026;16(71s): 68-79. DOI: 10.25258/ijddt.16.71s.9

1. Introduction

Pollution and pathogens represent dual challenges that humanity has struggled with for centuries. The combined effects of contaminated air, polluted water resources, and infectious agents have caused severe threats to both human health and environmental sustainability. Among various environmental issues, water pollution has emerged as one of the most serious global concerns due to the continuous release of industrial effluents, toxic chemicals, and hazardous organic compounds into natural water bodies [1-3]. Textile, pharmaceutical, cosmetic, leather, printing, and dye manufacturing industries discharge enormous quantities of colored wastewater containing synthetic dyes into aquatic ecosystems. These dye pollutants are highly stable, non-biodegradable, carcinogenic, and toxic in nature, thereby posing severe ecological and health-related problems.

Synthetic dyes are specifically designed to resist fading upon exposure to light, temperature, oxidizing agents, and microbial attack. Due to their complex aromatic molecular structures and high chemical stability, they persist in water bodies for extended periods. Even very small concentrations of dyes can impart intense coloration to water, thereby reducing light penetration, disturbing photosynthetic activity, and adversely affecting aquatic organisms.

Among the various synthetic dyes, Rhodamine 6G (Rh6G) has attracted significant attention because of its extensive industrial and technological applications. Rhodamine 6G is a fluorescent cationic xanthene dye extensively used in textile dyeing, fluorescence microscopy, biological staining, laser technologies, analytical chemistry, and sensor fabrication. However, prolonged exposure to Rhodamine 6G may result in skin irritation, eye damage, respiratory disorders, neurotoxicity, and carcinogenic effects. Therefore, the efficient removal and degradation of Rhodamine 6G from wastewater is of considerable environmental importance.

In recent years, metal oxide nanoparticles have gained remarkable scientific attention due to their exceptional applications in catalysis, environmental remediation, medicine, agriculture, electronics, optics, materials chemistry, and energy conversion systems [4-10]. Owing to their nanoscale dimensions, these nanoparticles exhibit unique optical, electrical, magnetic, photocatalytic, and physicochemical properties when compared to their bulk counterparts.

Several physical and chemical approaches such as sol-gel synthesis, co-precipitation, hydrothermal synthesis, thermal decomposition, microwave-assisted synthesis, combustion methods, and chemical reduction techniques have been employed for the preparation of metal oxide nanoparticles [11-13]. However, these conventional synthetic methods possess certain disadvantages including high energy consumption, elevated temperature requirements, utilization of toxic chemicals, generation of hazardous by-products, and high operational costs [14]. Consequently, the development of environmentally

benign and sustainable synthesis methods has become increasingly important.

Green synthesis approaches involving natural resources such as plant extracts, microbial extracts, algae, and agricultural waste materials have emerged as promising alternatives for nanoparticle synthesis [15]. Among these methods, plant extract-mediated synthesis has gained considerable popularity because it is simple, economical, eco-friendly, and highly efficient. Plant extracts contain diverse phytochemicals including flavonoids, alkaloids, tannins, polyphenols, terpenoids, proteins, sugars, vitamins, and organic acids that function as natural reducing, stabilizing, and capping agents during nanoparticle synthesis.

Copper oxide (CuO) nanoparticles have emerged as attractive semiconductor materials because of their low cost, high catalytic activity, chemical stability, and visible-light-responsive photocatalytic properties. CuO is a p-type semiconductor possessing a narrow indirect band gap of approximately 1.2–1.5 eV [16,17], making it highly suitable for visible-light-driven photocatalytic applications.

Due to these remarkable properties, CuO nanoparticles have found extensive applications in catalysis, sensors, lithium-ion batteries, antimicrobial coatings, environmental remediation, solar energy conversion, wastewater treatment, and photocatalytic degradation processes [18-31]. Compared to noble metal nanoparticles such as silver and gold, CuO nanoparticles provide a more economical and sustainable alternative for large-scale industrial and environmental applications.

Various plant extracts including Calotropis procera [32], Cassia auriculata [33], Tinospora cordifolia [34], Albizia lebbeck [35], and Bifurcaria bifurcata [36] have been successfully utilized for the green synthesis of CuO nanoparticles. The synthesis of CuO nanostructures in forms such as nanorods, nanowires, nanoflowers, nanoneedles, and nanoparticles further enhances their catalytic efficiency due to increased surface area and active reaction sites.

Tea waste is an abundant agro-industrial waste material rich in polyphenols, flavonoids, catechins, caffeine, and tannins. These bioactive compounds can effectively participate in the reduction and stabilization of nanoparticles during synthesis. Utilization of waste tea extract not only provides a sustainable synthesis route but also contributes toward waste management and circular economy principles [37,38].

Advanced Oxidation Technologies (AOTs) have emerged as highly effective approaches for the degradation of hazardous organic pollutants present in wastewater. Among them, heterogeneous photocatalysis has attracted immense attention because it enables complete mineralization of pollutants into harmless end products such as carbon dioxide and water without generating secondary pollutants. Visible-light-driven photocatalysis is particularly advantageous because sunlight can be utilized as an inexpensive and renewable energy source, thereby minimizing energy consumption and avoiding health hazards associated with ultraviolet irradiation.

During photocatalysis, highly reactive hydroxyl radicals (OH•) and superoxide radicals (O2•−) are generated on the photocatalyst surface. These reactive oxygen species possess strong oxidizing capability and can effectively degrade o\\rganic dye molecules into simpler, non-toxic products [39].

In the present investigation, the primary objective is the degradation of Rhodamine 6G dye using CuO nanoparticles synthesized through a green synthesis approach employing waste tea extract. The synthesized waste tea-mediated CuO nanoparticles (WT-CuO NPs) were comprehensively characterized using Fourier Transform Infrared Spectroscopy (FTIR), X-Ray Diffraction (XRD), High-Resolution Transmission Electron Microscopy (HR-TEM), Field Emission Scanning Electron Microscopy (FE-SEM), and Energy Dispersive X-ray Analysis (EDAX).

Furthermore, the photocatalytic degradation efficiency of Rhodamine 6G dye was investigated under visible light and natural sunlight irradiation. The effects of various experimental parameters including catalyst dosage, pH, dye concentration, and contact time were systematically evaluated in order to determine the optimum conditions for maximum photocatalytic degradation efficiency.

2. Experimental

2.1 Materials

All the reagents used in the present investigation were of analytical grade and utilized without any further purification. Copper nitrate trihydrate [Cu(NO3)2·3H2O] was procured from S.D. Fine Chemicals, while Rhodamine 6G dye was purchased from Hi-Media Laboratories, India. Waste tea was collected from local tea shops in the nearby market area and utilized for the synthesis of CuO nanoparticles.

Deionized water was used throughout the experimental work. All glassware employed during the investigation was thoroughly washed with distilled water and dried in a hot air oven maintained at 100°C for two hours prior to usage in order to avoid contamination.

The heating process during nanoparticle synthesis was carried out using a hot plate equipped with a magnetic stirrer, whereas centrifugation was performed using a REMI model centrifuge machine.

2.2 Preparation of Waste Tea Extract

The waste tea extract was prepared by mixing 2 g of waste tea with 100 mL of distilled water. The resulting mixture was heated at 353 K for 60 minutes using a water bath. After completion of the heating process, the extract was filtered under vacuum conditions to remove solid residues.

The obtained filtrate was subsequently stored at a temperature range of 5–10°C for further utilization in the synthesis of CuO nanoparticles.

2.3 Synthesis of CuO Nanoparticles

A 0.10 mol/L solution of copper nitrate trihydrate [Cu(NO3)2·3H2O] was introduced into the waste tea extract in a 1:2 volume ratio. After the addition of copper salt, the reaction mixture was continuously stirred and heated at 80–90°C for 6–8 hours. The formation of waste

tea-mediated CuO nanoparticles (WT-CuO NPs) was indicated by the appearance of black-coloured CuO nanoparticles in the solution containing Cu (II) ions and tea extract. The obtained mixture was subsequently centrifuged for 15 minutes, during which the supernatant liquid was discarded, and the solid residue was washed three times with distilled water to remove residual salts and tea-derived compounds from the nanoparticle surface. Following the final washing step, the CuO nanoparticles were subjected to another cycle of centrifugation, after which the liquid portion was removed and the nanoparticles were dried in a hot air oven for further characterization and photocatalytic studies [40].

2.4 Photocatalytic Degradation Study

Rhodamine 6G was utilized as a model organic dye for investigating the photocatalytic activity of waste tea-mediated CuO nanoparticles (WT-CuO NPs). All photocatalytic degradation experiments were carried out under visible light irradiation using a 100 W tungsten lamp as well as under natural sunlight at room temperature. The catalyst dosage was maintained at 50 mg, while the dye concentration was fixed at 50 ppm throughout the study.

Initially, 50 mL of Rhodamine 6G dye solution was treated individually with 50 mg of the synthesized WT-CuO nanoparticle catalyst. Prior to visible light irradiation, all photocatalyst-containing solutions were sonicated for one minute in order to achieve maximum dispersion of nanoparticles within the dye solution.

The photocatalytic degradation process was monitored using a UV-Visible spectrophotometer at the maximum absorbance wavelength of Rhodamine 6G dye (λmax ≈ 526 nm). Absorbance measurements were recorded at 15-minute intervals over a total contact period of 120 minutes.

The degradation efficiency (η) and pseudo-first-order rate constant (k) for the photocatalytic degradation process were determined using Equations (1) and (2), respectively.

Degradation% (η) = (C0−Ct)/C0×100

ln(C0/Ct) = kt

Here, C0 and Ct represent the initial and final absorbance values of the dye solution at λmax, while k denotes the pseudo-first-order rate constant(sec-1). Similar photocatalytic degradation studies were also performed both in the presence and absence of the photocatalyst under visible light and natural sunlight irradiation conditions

.

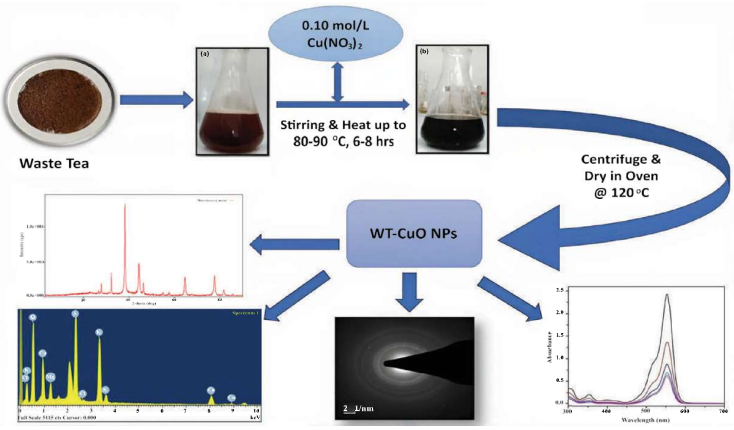

Fig. (1). Schematic diagram of WT_CuO nanoparticles.

3. Results and Discussion

3.1Characterization of Waste Tea-mediated CuO Nano- particles

3.1.1 FTIR Analysis

FTIR spectroscopy was employed to characterize and identify the phytochemical constituents present in the waste tea extract as well as the synthesized CuO nanoparticles. The FTIR spectra of waste tea extract and synthesized waste tea-mediated CuO nanoparticles (WT-CuO NPs) revealed noticeable peak shifts after the reaction between copper nitrate and tea waste extract, confirming the involvement of biomolecules in nanoparticle synthesis and stabilization (Fig. (2)).

The broad absorption band observed around 3310.7 cm−1 corresponds to the stretching vibration of the hydroxyl (O–H) functional group present in alcohols and phenolic compounds. The sharp absorption peaks appearing in the region between 1700 and 1000 cm−1 indicate the presence of various organic functional groups derived from phytochemicals present in the tea extract.

The IR absorption band around 1611.2 cm−1 is attributed to the aromatic bending vibration of alkene (C=C) groups. The sharp peak observed at 1342.3 cm−1 corresponds to the deformation vibration of the C–H bond associated with alkane groups such as CH3 and CH2. The absorption peak at 1038.0 cm−1 is assigned to the stretching vibration of the C–O functional group of primary and secondary alcohols.

Furthermore, the peaks observed in the region between 900–700 cm−1 correspond to the C–H out-of-plane bending vibrations characteristic of aromatic phenolic compounds. A strong absorption peak observed around 600 cm−1 confirms the formation of CuO nanoparticles and is attributed to Cu–O stretching vibrations, thereby indicating the successful synthesis of copper oxide nanoparticles [24].

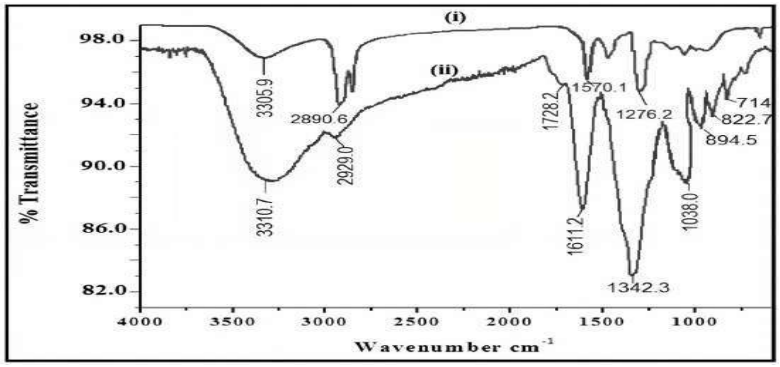

Fig. (2). Fourier Transform Infrared spectroscopy (FTIR) spectra of (i) Tea waste extract; (ii) Tea waste-mediated CuO nanoparticles.

3.1.2 XRD Analysis

The XRD pattern of the newly synthesized WT-CuO nanoparticles (Fig.3) was analysed to investigate their crystalline nature. The prominent diffraction peaks observed at 2θ values of 28°, 32°, 38°, 44°, 64°, and 77° correspond to the (100), (110), (111), (200), (210), and (220) Bragg reflection planes, respectively. All diffraction peaks were well indexed to the monoclinic crystal structure of waste tea-mediated CuO nanoparticles and showed good agreement with the JCPDS file No. 45-0937. Moreover, the presence of sharp and distinct peaks in the diffraction pattern confirms the crystalline nature of the synthesized WT-CuO nanoparticles (Fig. (3)).

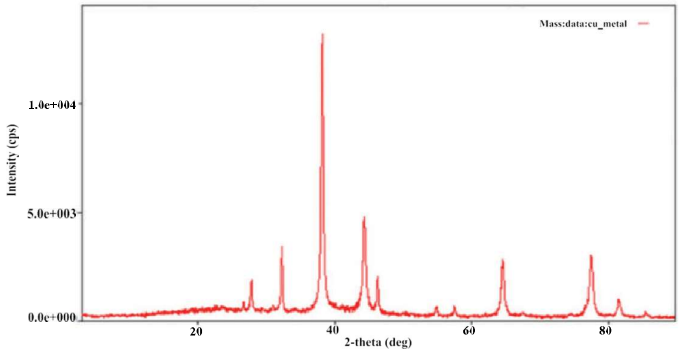

Fig. (3). XRD spectra of WT-CuO NPs.

3.1.3 FE-SEM and EDAX Analysis

The SEM image of WT-CuO nanoparticles (Fig. 4a) revealed that the particles were nearly spherical, uniformly distributed, and showed slight aggregation. This aggregation may be attributed to the capping effect of phenolic compounds present during the synthesis process [16].

The EDX spectrum of WT-CuO nanoparticles (Fig. 4b) displayed strong characteristic peaks for copper (Cu) and oxygen (O) at 0.9 and 8.1 keV, and 0.5 keV, respectively. The absence of additional impurity peaks indicates the high purity of the synthesized WT-CuO nanoparticles. The elemental composition analysis showed that the nanoparticles contained 80.14 wt% Cu and 17.45 wt% O. In addition, the atomic percentages of Cu and O were found to be 48.56% and 44.24%, respectively. These findings are in good agreement with previously reported studies on CuO nanoparticles.

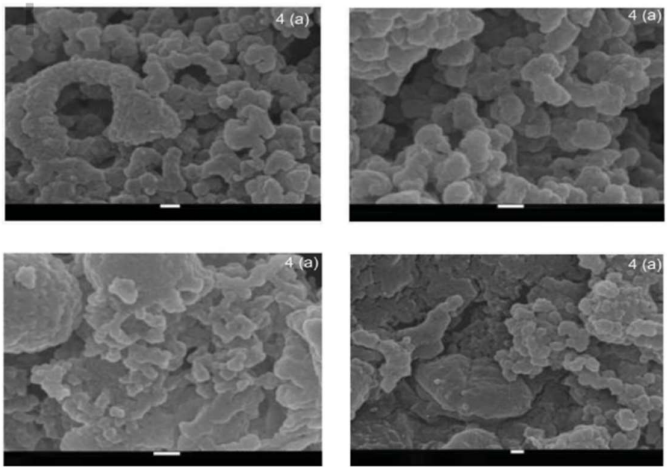

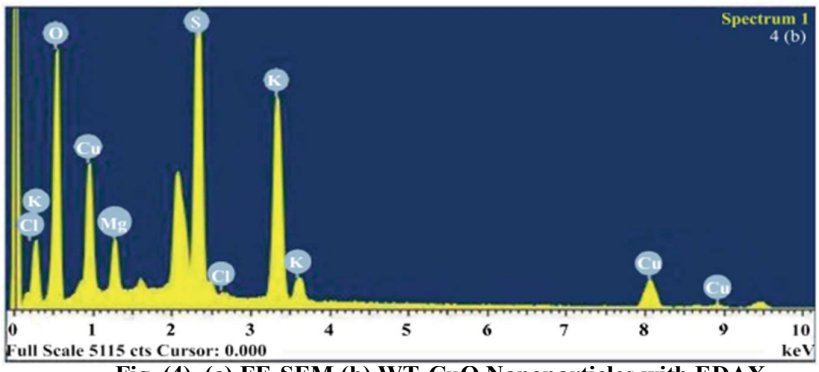

Fig. (4). (a) FE-SEM (b) WT-CuO Nanoparticles with EDAX

3.1.4 HR-TEM Analysis

The TEM images of WT-CuO nanoparticles presented in Fig. 5 revealed that the synthesized particles were mainly spherical in shape, with a few slightly agglomerated hexagonal particles. The particle size distribution histogram indicated that the size of the nanoparticles ranged from 20 to 40 nm. Most of the particles were found within the 20–25 nm range, and the average particle size was determined to be approximately 22 nm.

The inset SAED (Selected Area Electron Diffraction) patterns shown in the micrographs exhibited distinct concentric rings, confirming the polycrystalline nature of the synthesized WT-CuO nanoparticles [41,42].

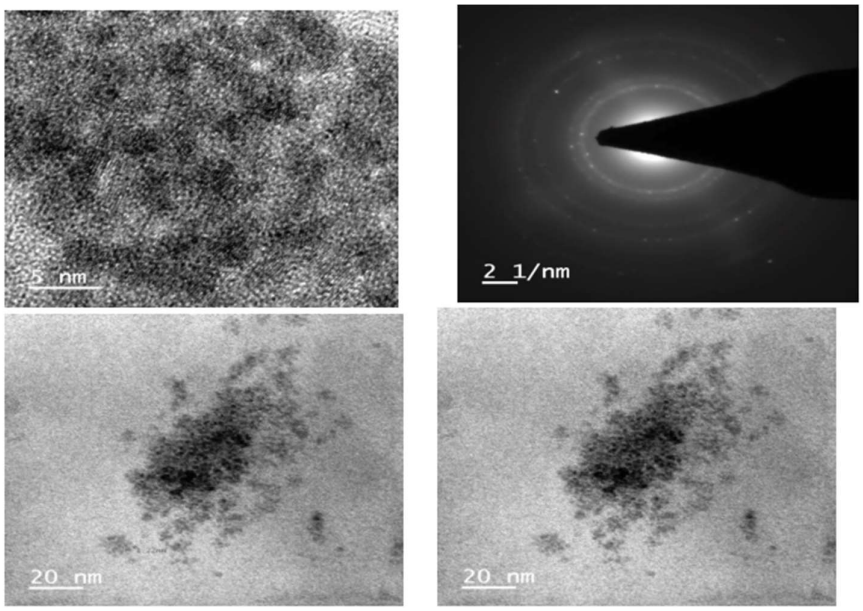

Fig. (5). HR-TEM images of WT-CuO Nanoparticles

3.2 Photocatalytic Degradation of Rhodamine 6G Dye

The photocatalytic activity of the synthesized nanostructures was evaluated by studying the degradation of Rhodamine 6G (Rh6G) dye under UV-visible light irradiation. Visual observation indicated that the intensity of the dye color gradually decreased with increasing irradiation time. The absorbance spectrum of Rh6G exhibited a characteristic absorption peak around 526 nm in the visible region, which is attributed to the chromophoric group responsible for the dye's color.

The absorbance of the dye solution containing the photocatalyst was monitored at different illumination intervals. A gradual decrease in the absorbance peak intensity was observed with increasing exposure time. According to the Lambert–Beer law, the reduction in absorbance corresponds to a decrease in dye concentration in the solution. The continuous decline in the characteristic absorption peak confirms the photodegradation and decolorization of Rh6G dye under UV-visible light irradiation.

3.2.1 Influence of Various Experimental Parameters on the Adsorption of Rhodamine B (RhB) Dye by WT-CuO Nanoparticles

3.2.1.1 Effect of Catalyst Dosage

The proposed theory suggests that the efficiency of dye removal using an adsorbent material mainly depends on the surface area of the adsorbent exposed to the dye solution. To support this concept, experiments were carried out using reaction vessels of different sizes. It was observed that larger containers with greater bottom surface areas increased the exposed area of the adsorbent, resulting in a higher percentage of Rhodamine 6G (Rh6G) dye removal. This indicates that a larger exposed surface allows more dye molecules to interact with the adsorbent, thereby enhancing the adsorption process (Fig. 6).

In the present study, however, beakers of the same size were used throughout the experiment. Under these conditions, once the adsorbent reached its maximum exposed surface area, the addition of more adsorbent only increased the thickness of the adsorbent layer rather than the effective exposed area. Consequently, the extra adsorbent did not significantly improve the percentage of dye removal.

The experimental results demonstrated that 50 mg of adsorbent was the optimum amount for achieving the maximum removal efficiency of Rhodamine 6G dye. This finding suggests the existence of an ideal adsorbent-to-dye ratio for effective dye removal. Overall, the study emphasizes the importance of optimizing the exposed surface area of the adsorbent to achieve efficient removal of Rhodamine 6G from aqueous solutions.

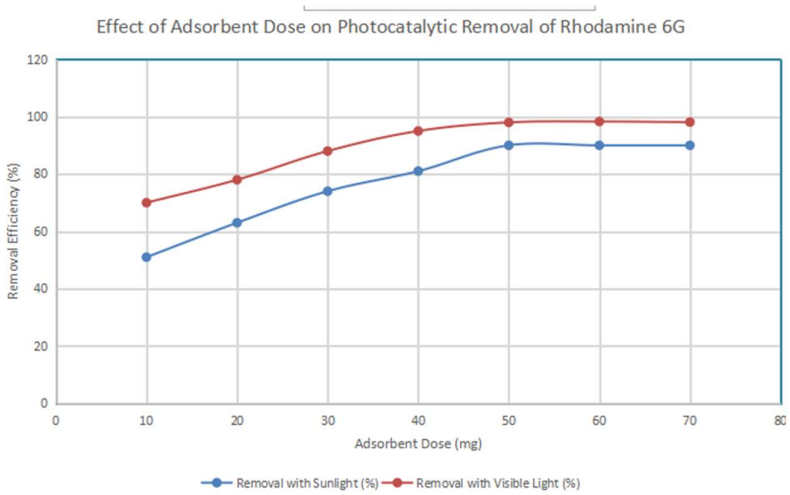

Fig. (6). Effect of adsorbent dosage on the adsorption of Rhodamine 6G by WT-CuO nanoparticles.

3.2.1.2 Effect of pH

Fig. 7 graphically illustrates the adsorption behavior of Rhodamine 6G (Rh6G) dye at different pH values. The results demonstrate that the adsorption efficiency of Rh6G gradually increased as the pH was raised from 4.0 to 8.0. However, beyond pH 8.0, the percentage of dye removal started to decrease. This behavior can be explained by the variation in the surface charge properties of CuO nanoparticles with changing pH conditions.

As shown in Fig. 7, the surface charge of CuO nanoparticles changes from positive to negative with increasing pH, resulting in enhanced electrostatic interactions between the adsorbent surface and Rhodamine 6G dye molecules. Consequently, the percentage of dye removal increased significantly as the pH increased from 2 to 8. In contrast, a further increase in pH from 8 to 9 caused a reduction in dye removal efficiency.

The maximum adsorption capacity for Rhodamine 6G was observed at pH 8.0, indicating that CuO nanoparticles possess the highest affinity toward the dye under these conditions. The study further revealed that the highest degradation efficiency of Rhodamine 6G achieved using CuO nanoparticles was approximately 98.65% under visible light irradiation and 88.90% under sunlight conditions. These findings highlight the excellent potential of CuO nanoparticles as effective photocatalysts for the degradation of Rhodamine 6G dye under different illumination sources.

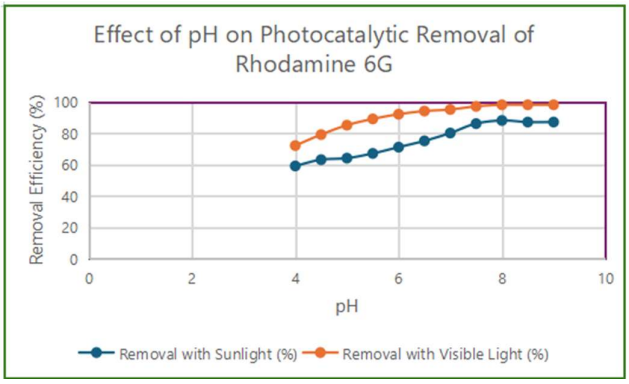

Fig. (7). Effect of pH on the adsorption of Rhodamine 6G by WT-CuO nanoparticle.

3.2.1.3 Effect of Dye Concentration

The experimental results demonstrate a strong relationship between the initial concentration of Rhodamine 6G (Rh6G) dye and its adsorption behavior. As the initial concentration of Rh6G increased from 20 ppm to 50 ppm, the equilibrium adsorption capacity also increased. This behavior can be explained by the higher mass transfer driving force generated at elevated dye concentrations, which promotes greater adsorption of dye molecules onto the adsorbent surface.

However, the percentage of dye removal showed a decreasing trend with an increase in the initial dye concentration. This decrease may be attributed to the limited number of active adsorption sites available on the surface of the adsorbent. At higher dye concentrations, more dye molecules compete for the available adsorption sites, resulting in a lower overall percentage of dye removal.

As illustrated in Fig. 8, the maximum degradation efficiency achieved using waste tea-mediated CuO nanoparticles was approximately 98.71% for a 50 ppm Rhodamine 6G dye solution under visible light irradiation. Similarly, under sunlight exposure, the degradation efficiency reached about 89.95% for the same dye concentration. These findings confirm the effectiveness of waste tea-mediated CuO nanoparticles as promising photocatalysts for the degradation of Rhodamine 6G dye, especially under visible light conditions.

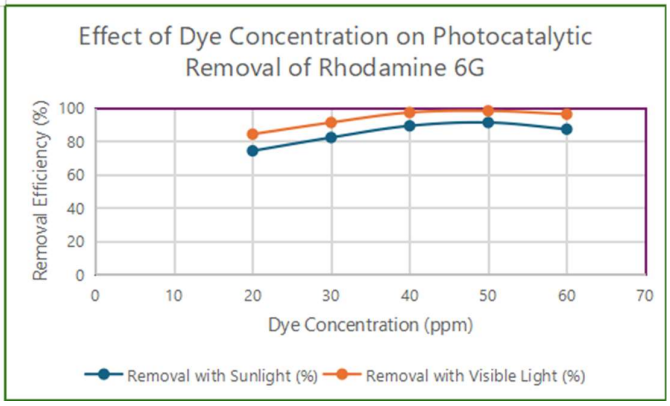

Fig. (8). Effect of concentration on the adsorption of Rhodamine 6G by WT-CuO Nanoparticles

3.2.1.4 Effect of Contact Time

Contact time is one of the most influential parameters affecting the adsorption efficiency of dyes from aqueous solutions. In the present study, adsorption experiments were carried out at predetermined time intervals to evaluate the effect of contact time on the removal of Rhodamine 6G (Rh6G) dye. The variation in the percentage of dye removal with contact time is illustrated in Fig. 9. The results reveal a positive correlation between contact time and adsorption efficiency, with the percentage removal of Rhodamine 6G increasing as the contact duration increased. This indicates that sufficient interaction time between the adsorbent and dye molecules is essential for achieving effective adsorption.

The adsorption of Rhodamine 6G was rapid during the initial stages of the experiment due to the abundance of vacant active sites available on the surface of the adsorbent. As adsorption progressed, the rate of dye removal gradually decreased because the easily accessible adsorption sites became occupied. Subsequently, the adsorption process was controlled by the slower diffusion of Rhodamine 6G molecules into the internal pores and deeper layers of the adsorbent. This reduction in adsorption rate at longer contact times is attributed to intraparticle diffusion and the gradual attainment of adsorption equilibrium.

The maximum adsorption efficiency was achieved after 90 minutes of contact time using WT-CuO nanoparticles, with a Rhodamine 6G removal efficiency of approximately 98.90%. Beyond this contact time, no significant increase in dye removal was observed, indicating that equilibrium had been established between the adsorbate and the adsorbent. These findings demonstrate that contact time plays a crucial role in the adsorption process and that a 90-minute equilibrium time is sufficient for the efficient removal of Rhodamine 6G. The observed adsorption behavior highlights the combined influence of surface adsorption and diffusion mechanisms in determining the overall adsorption performance.

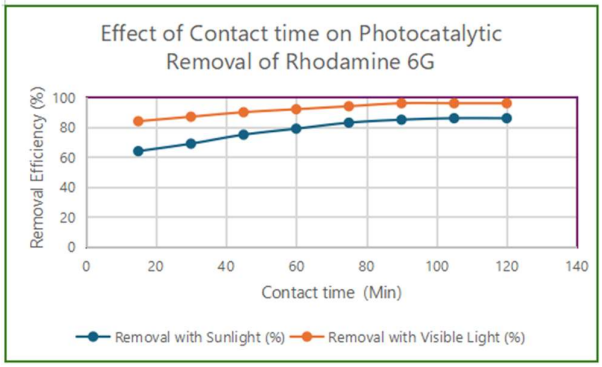

3.2.2 Possible Mechanism of Rhodamine 6G Degradation

When CuO nanoparticles are dispersed in an aqueous solution containing Rhodamine 6G (Rh6G) dye and exposed to UV-Visible light, a sequence of photocatalytic reactions is initiated. Photons with energy equal to or greater than the bandgap of CuO excite electrons from the valence band to the conduction band, resulting in the generation of electron-hole pairs. These photogenerated charge carriers are responsible for the photocatalytic activity of the nanoparticles. The holes oxidize water molecules or hydroxide ions adsorbed on the catalyst surface to produce highly reactive hydroxyl radicals, while the excited electrons reduce dissolved oxygen molecules to form superoxide radicals. These reactive oxygen species further participate in a series of reactions, producing additional hydroxyl radicals that possess strong oxidative potential. The generated hydroxyl and superoxide radicals effectively attack and decompose Rhodamine 6G dye molecules into smaller, non-toxic products such as carbon dioxide, water, and inorganic ions without forming harmful intermediate compounds. This photocatalytic degradation mechanism demonstrates the excellent efficiency of CuO nanoparticles for the removal of Rhodamine 6G and highlights their potential as an environmentally friendly and sustainable catalyst for wastewater treatment.

The steps that are believed to be involved in the formation of free radicals are:

$CuO + h\nu \rightarrow CuO (e\text{-}cb + h+vb)$
$H2O + h+vb \rightarrow OH^* + H+$
$O2 + e^- \rightarrow O2^{*-}$
$O2- + H2O \rightarrow H2O2$
$OH^* + Rh6G \rightarrow$ degraded products

The comparison study is shown in Table 1

Photocatalysts	Plant Name	Dye	Light Source	Time(min)	Degradation %	References
CuO	Artabotrys hexapetalus	Rhodamine B	Visible light	180	91	[43]
CuO	Euphorbia maculata	Rhodamine B	UV light	60	89	[44]
CuO	ferulago angulata	Rhodamine B	Visible light	150	83	[45]
CuO	Murrya koenigi	Reactive Black	Visible light	10	80	[46]
CuO	Scoparia dulsis	Methyl Orange	125 W UV lamp	180	94.4	[47]
CuO	Ruellia tuberosa	Crystal Violet	Sunlight	120	100	[48]
CuO	Madhuca longifolia	Methylene Blue	Visible light	150	77	[49]
CuO	Banana Peel	Congo Red	Sunlight	60	90	[50]
WT-CuO	Waste Tea	RhB	Visible	90	98.90	[40]
WT-CuO	Waste Tea	Rh6G	Visible	90	95.90	Present work

Conclusion

Waste tea extract was successfully employed as a green reducing and stabilizing agent for the synthesis of highly crystalline CuO nanoparticles with excellent photocatalytic activity toward Rhodamine 6G (Rh6G) degradation. Under the optimized conditions of pH 8, 50 mg catalyst dosage, 50 ppm Rh6G concentration, and 90 min irradiation time, the synthesized WT-CuO nanoparticles achieved a maximum degradation efficiency of 95.90% under visible-light irradiation, compared with 89.95% under natural sunlight irradiation, demonstrating the superior photocatalytic performance of visible light while confirming the practical applicability of renewable solar energy for dye degradation. Compared with previously reported green-synthesized CuO photocatalysts, the waste tea-derived CuO nanoparticles exhibited competitive photocatalytic performance using an inexpensive and sustainable biomass precursor. Overall, the excellent degradation efficiency achieved for Rhodamine 6G under both visible-light and natural sunlight irradiation highlights the potential of waste tea-derived CuO nanoparticles as low-cost, environmentally benign, and highly efficient photocatalysts for the treatment of Rhodamine 6G-contaminated wastewater and other dye-bearing industrial effluents.

References:

1. Kumar A, Pandey G. A review on the factors affecting the photocatalytic degradation of hazardous materials. Materials Science and Engineering International Journal. 2017;1(3):1–10. DOI: https://doi.org/10.15406/mseij.2017.01.00018
2. Phaltane SA, Vanalakar SA, Bhat TS, Patil PS, Sartale SD, Kadam LD. Photocatalytic degradation of methylene blue by hydrothermally synthesized CZTS nanoparticles. Journal of Materials Science: Materials in Electronics. 2017;28(11):8186–8191. DOI: https://doi.org/10.1007/s10854-017-6527-0

3. Rochkind M, Pasternak S, Paz Y. Using dyes for evaluating photocatalytic properties: A critical review. Molecules. 2014;20(1):88–110. DOI: https://doi.org/10.3390/molecules20010088
4. Chari N, Felix L, Davoodbasha M, Ali SA, Nooruddin T. In vitro and in vivo antibiofilm effect of copper nanoparticles against aquaculture pathogens. Biocatalysis and Agricultural Biotechnology. 2017;10:336–341.DOI: https://doi.org/10.1016/j.bcab.2017.04.013
5. Dong Y, Jiang X, Mo J, Zhou Y, Zhou J. Hollow CuO nanoparticles in carbon microspheres prepared from cellulose-cuprammonium solution as anode materials for Li-ion batteries. Chemical Engineering Journal. 2020;381:122614. DOI: https://doi.org/10.1016/j.cej.2019.122614
6. Fuku X, Modibedi M, Mathe M. Green synthesis of Cu/Cu_2O/CuO nanostructures and the analysis of their electrochemical properties. SN Applied Sciences. 2020;2(5):902. DOI: https://doi.org/10.1007/s42452-020-2704-5
7. Pradeep T, Anshup. Noble metal nanoparticles for water purification: A critical review. Thin Solid Films. 2009;517(24):6441–6478. DOI: https://doi.org/10.1016/j.tsf.2009.03.195
8. Sathiyavimal S, Vasantharaj S, Bharathi D, et al. Biogenesis of copper oxide nanoparticles (CuONPs) using Sida acuta and their incorporation over cotton fabrics to prevent the pathogenicity of Gram-negative and Gram-positive bacteria. Journal of Photochemistry and Photobiology B: Biology. 2018;188:126–134. DOI: https://doi.org/10.1016/j.jphotobiol.2018.09.014
9. Sone BT, Diallo A, Fuku XG, Gurib-Fakim A, Maaza M. Biosynthesized CuO nano-platelets: Physical properties & enhanced thermal conductivity nanofluidics. Arabian Journal of Chemistry. 2020;13(1):160–170. DOI: https://doi.org/10.1016/j.arabjc.2017.03.004
10. Zeid EFA, Ibrahem IA, Mohamed WAA, Ali AM. Study the influence of silver and cobalt on the photocatalytic activity of copper oxide nanoparticles for the degradation of methyl orange and real wastewater dyes. Materials Research Express. 2020;7(2):026201 DOI: https://doi.org/10.1088/2053-1591/ab7400
11. Khashan KS, Sulaiman GM, Abdulameer FA. Synthesis and antibacterial activity of CuO nanoparticles suspension induced by laser ablation in liquid. Arabian Journal for Science and Engineering. 2016;41(1):301–310. DOI: https://doi.org/10.1007/s13369-015-1733-7
12. Musić S, Dragčević Đ, Maljković M, Popović S. Influence of chemical synthesis on the crystallization and properties of zinc oxide. Materials Chemistry and Physics. 2003;77(2):521–530. DOI: https://doi.org/10.1016/S0254-0584(02)00088-3
13. Wilson N. Nanoparticles: Environmental problems or problem solvers. BioScience. 2018;68(4):241–246. DOI: https://doi.org/10.1093/biosci/biy015
14. Chavali MS, Nikolova MP. Metal oxide nanoparticles and their applications in nanotechnology. SN Applied Sciences. 2019;1(6):607. DOI: https://doi.org/10.1007/s42452-019-0592-3
15. Singh J, Dutta T, Kim KH, Rawat M, Samddar P, Kumar P. Green synthesis of metals and their oxide nanoparticles: Applications for environmental remediation. Journal of Nanobiotechnology. 2018;16(1):84. DOI: https://doi.org/10.1186/s12951-018-0408-4
16. Prabhash PG, Nair SS. Synthesis of copper quantum dots by chemical reduction method and tailoring of its band gap. AIP Advances. 2016;6(5):055003. DOI: https://doi.org/10.1063/1.4948747
17. Singh PK, Kumar P, Hussain M, Das AK, Nayak GC. Synthesis and characterization of CuO nanoparticles using strong base electrolyte through electrochemical discharge process. Bulletin of Materials Science. 2016;39(2):469–478. DOI: https://doi.org/10.1007/s12034-016-1159-1
18. Logpriya S, Bhuvaneshwari V, Vaidehi D, et al. Preparation and characterization of ascorbic acid-mediated chitosan–copper oxide nanocomposite for antimicrobial, sporicidal and biofilm-inhibitory activity. Journal of Nanostructure Chemistry. 2018;8(3):301–309. DOI: https://doi.org/10.1007/s40097-018-0273-6
19. Botsa SM, Basavaiah K. Removal of nitrophenols from wastewater by monoclinic CuO/rGO nanocomposite. Nanotechnology for Environmental Engineering. 2019;4(1):1–7. DOI: https://doi.org/10.1007/s41204-018-0045-z
20. Botsa SM, Dharmasoth R, Basavaiah K. A facile synthesis of Cu_2O and CuO nanoparticles via sonochemical assisted method. Current Nanoscience. 2019;15(2):209–213 DOI: https://doi.org/10.2174/1573413714666180530085447
21. Chaudhary K, Subodh, Prakash K, Mogha NK, Masram DT. Fruit waste (Pulp) decorated CuO nanoflowers as promising platform for enhanced catalytic response and its peroxidase mimics evaluation. Arabian Journal of Chemistry. 2020;13(4):4869–4881. DOI: https://doi.org/10.1016/j.arabjc.2019.09.007
22. Chowdhury R, Khan A, Rashid MH. Green synthesis of CuO nanoparticles using Lantana camara flower extract and their potential catalytic activity towards the aza-Michael

reaction. RSC Advances. 2020;10(24):14374–14385. DOI: https://doi.org/10.1039/D0RA01479F

23. Kayalvizhi S, Sengottaiyan A, Selvankumar T, Senthilkumar B, Sudhakar C, Selvam K. Eco-friendly cost-effective approach for synthesis of copper oxide nanoparticles for enhanced photocatalytic performance. Optik. 2020;202:163507. DOI: https://doi.org/10.1016/j.ijleo.2019.163507
24. Rehana D, Mahendiran D, Kumar RS, Rahiman AK. Evaluation of antioxidant and anticancer activity of copper oxide nanoparticles synthesized using medicinally important plant extracts. Biomedicine & Pharmacotherapy. 2017;89:1067–1077. DOI: https://doi.org/10.1016/j.biopha.2017.02.101
25. Renuga D, Jeyasundari J, Athithan SAS, Jacob BAY. Synthesis and characterization of copper oxide nanoparticles using Brassica oleracea var. italica extract for its antifungal application. Materials Research Express. 2020;7(4):045007. DOI: https://doi.org/10.1088/2053-1591/ab7b94
26. Scuderi V, Amiard G, Boninelli S, et al. Photocatalytic activity of CuO and Cu_2O nanowires. Materials Science in Semiconductor Processing. 2016;42:89–93. DOI: https://doi.org/10.1016/j.mssp.2015.08.008
27. Sree GS, Botsa SM, Reddy BJM, Ranjitha KVB. Enhanced UV–Visible triggered photocatalytic degradation of Brilliant Green by reduced graphene oxide based NiO and CuO ternary nanocomposite and their antimicrobial activity. Arabian Journal of Chemistry. 2020;13(4):5137–5150. DOI: https://doi.org/10.1016/j.arabjc.2020.02.012
28. Tadjarodi A, Akhavan O, Bijanzad K. Photocatalytic activity of CuO nanoparticles incorporated in mesoporous structure prepared from bis(2-aminonicotinato) copper(II) microflakes. Transactions of Nonferrous Metals Society of China. 2015;25(11):3634–3642. DOI: https://doi.org/10.1016/S1003-6326(15)64004-3
29. Turakhia B, Divakara MB, Santosh MS, Shah S. Green synthesis of copper oxide nanoparticles: A promising approach in the development of antibacterial textiles. Journal of Coatings Technology and Research. 2020;17(2):531–540. DOI: https://doi.org/10.1007/s11998-019-00303-5
30. Wang C, Higgins D, Wang F, et al. Controlled synthesis of micro/nanostructured CuO anodes for lithium-ion batteries. Nano Energy. 2014;9:334–344. DOI: https://doi.org/10.1016/j.nanoen.2014.08.009
31. Rao MP, Sathishkumar P, Mangalaraja RV, Asiri AM, Sivashanmugam P, Anandan S. Simple and low-cost synthesis of CuO nanosheets for visible-light-driven photocatalytic degradation of textile dyes. Journal of Environmental Chemical Engineering. 2018;6(2):2003–2010. DOI: https://doi.org/10.1016/j.jece.2018.03.008
32. Dubey S, Sharma YC. Calotropis procera mediated one-pot green synthesis of cupric oxide nanoparticles (CuO-NPs) for adsorptive removal of Cr(VI) from aqueous solutions. Applied Organometallic Chemistry. 2017;31(12):e3849. DOI: https://doi.org/10.1002/aoc.3849
33. Shi LB, Tang PF, Zhang W, Zhao YP, Zhang LC, Zhang H. Green synthesis of CuO nanoparticles using Cassia auriculata leaf extract and in vitro evaluation of their biocompatibility with rheumatoid arthritis macrophages (RAW 264.7). Tropical Journal of Pharmaceutical Research. 2017;16(1):185–192. DOI: https://doi.org/10.4314/tjpr.v16i1.25
34. Udayabhanu, Nethravathi PC, Kumar PMA, et al. Tinospora cordifolia mediated facile green synthesis of cupric oxide nanoparticles and their photocatalytic, antioxidant and antibacterial properties. Materials Science in Semiconductor Processing. 2015;33:81–88. DOI: https://doi.org/10.1016/j.mssp.2015.01.034
35. Jayakumarai G, Gokulpriya C, Sudhapriya R, Sharmila G, Muthukumaran C. Phytofabrication and characterization of monodisperse copper oxide nanoparticles using Albizia lebbeck leaf extract. Applied Nanoscience. 2015;5(8):1017–1021. DOI: https://doi.org/10.1007/s13204-015-0402-1
36. Abboud Y, Saffaj T, Chagraoui A, et al. Biosynthesis, characterization and antimicrobial activity of copper oxide nanoparticles (CONPs) produced using brown alga extract (Bifurcaria bifurcata). Applied Nanoscience. 2014;4(5):571–576. DOI: https://doi.org/10.1007/s13204-013-0233-x
37. Mampilly RB, Pathan A, Bhasin CP. Iron capped spent tea leaves as nano-adsorbent for removal of Eriochrome Black T from aqueous phase. Asian Journal of Chemistry. 2021;34(7):1814–1820. DOI: https://doi.org/10.14233/ajchem.2022.23776
38. Mampilly RB, Pathan A, Bhasin CP. Visible light-assisted degradation of malachite green dye using waste tea-mediated zinc nanoparticles. International Journal of Thin Film Science and Technology. 2023;12(1):39–51 DOI: https://doi.org/10.18576/ijtfst/120
39. Hoffmann MR, Martin ST, Choi W, Bahnemann DW. Environmental applications of semiconductor photocatalysis. Chemical Reviews. 1995;95(1):69–96. DOI: https://doi.org/10.1021/cr00033a004
40. .Mampilly RB, Pathan A, Bhasin CP. Utilization of Low-Cost Waste Tea-Derived CuO Nanoparticles for Enhanced

Photocatalytic Decomposition of Rhodamine B Dye Under Visible Light Irradiation. Current Nanomaterials, 2025, 10, 473-484 DOI: 10.2174/0124054615218191240416050232

41. Zaman MB, Chandel T, Poolla R. Hydrothermal synthesis of Cu_2FeSnS_4 anisotropic nanoarchitectures: Controlled morphology for enhanced photocatalytic performance. Materials Research Express. 2019;6(7):075058. DOI: https://doi.org/10.1088/2053-1591/ab1797
42. Zaman BM, Mir RA, Poolla R. Growth and properties of solvothermally derived highly crystalline Cu_2ZnSnS_4 nanoparticles for photocatalytic and electrocatalytic applications. International Journal of Hydrogen Energy. 2019;44(41):23023–23033. DOI: https://doi.org/10.1016/j.ijhydene.2019.07.026
43. Haseena S, Shanavas S, Duraimurugan J, et al. Investigation on photocatalytic and antibacterial ability of green treated copper oxide nanoparticles using Artabotrys hexapetalus and Bambusa vulgaris plant extract. Materials Research Express. 2019;6(12):125064. DOI: https://doi.org/10.1088/2053-1591/ab59a9
44. Pakzad K, Alinezhad H, Nasrollahzadeh M. Green synthesis of $Ni@Fe_3O_4$ and CuO nanoparticles using Euphorbia maculata extract as photocatalysts for the degradation of organic pollutants under UV irradiation. Ceramics International. 2019;45(14):17173–17182 DOI: https://doi.org/10.1016/j.ceramint.2019.05.272
45. Shayegan Mehr E, Sorbiun M, Ramazani A, Fardood TS. Plant-mediated synthesis of zinc oxide and copper oxide nanoparticles using Ferulago angulata extract and comparison of their photocatalytic degradation of Rhodamine B under visible light irradiation. Journal of Materials Science: Materials in Electronics. 2018;29(2):1333–1340.DOI: https://doi.org/10.1007/s10854-017-8039-3
46. Anandhavalli N, Mol B, Manikandan S, Anusha N, Ponnusami V, Rajan KS. Green synthesis of cupric oxide nanoparticles using the water extract of Murraya koenigii and its photocatalytic activity. Asian Journal of Chemistry. 2015;27(7):2523–2526.DOI: https://doi.org/10.14233/ajchem.2015.17966
47. Navada KM, Nagaraja GK, D'Souza JN, Kouser S, Ranjitha R, Manasa DJ. Phyto-assisted synthesis and characterization of Scoparia dulcis L. leaf extract mediated porous nano CuO photocatalysts and its anticancer behavior. Applied Nanoscience. 2020;10(11):4221–4240.DOI: https://doi.org/10.1007/s13204-020-01536-2
48. Vasantharaj S, Sathiyavimal S, Saravanan M, et al. Synthesis of eco-friendly copper oxide nanoparticles for fabrication over textile fabrics: Characterization of antibacterial activity and dye degradation potential. Journal of Photochemistry and Photobiology B: Biology. 2019; 191:143–149. DOI: https://doi.org/10.1016/j.jphotobiol.2018.12.026
49. Das P, Ghosh S, Ghosh R, Dam S, Baskey M. Madhuca longifolia plant mediated green synthesis of cupric oxide nanoparticles: A promising environmentally sustainable material for wastewater treatment and efficient antibacterial agent. Journal of Photochemistry and Photobiology B: Biology. 2018; 189:66–73. DOI: https://doi.org/10.1016/j.jphotobiol.2018.09.023
50. Aminuzzaman M, Kei LM, Liang WH. Green synthesis of copper oxide (CuO) nanoparticles using banana peel extract and their photocatalytic activities. AIP Conference Proceedings. 2018;020016.. DOI: 10.2174/0124054615218191240416050232